THE JOURNAL OF PHYSICAL CHEMISTRY Letters

Letter

Cite This: J. Phys. Chem. Lett. 2018, 9, 6350−6355

pubs.acs.org/JPCL

Electronic State Mixing Controls the Photoreactivity of a Rhodopsin with all-*trans* Chromophore Analogues

Madushanka Manathunga,[†] Xuchun Yang,[†] and Massimo Olivucci*[,†,¶,‡]

[†]Department of Chemistry, Bowling Green State University, Bowling Green, Ohio 43403, United States

[¶]Dipartimento di Biotecnologie, Chimica e Farmacia, Università di Siena, via A. Moro 2, I-53100 Siena, Italy

[‡]Institut de Physique et Chimie des Matériaux de Strasbourg, UMR 7504 Université de Strasbourg-CNRS, F-67034 Strasbourg, France

Supporting Information

ABSTRACT: Rhodopsins hosting synthetic retinal protonated Schiff base analogues are important for developing tools for optogenetics and high-resolution imaging. The ideal spectroscopic properties of such analogues include long-wavelength absorption/emission and fast/hindered photoisomerization. While the former may be achieved, for instance, by elongating the chromophore π-system, the latter requires a detailed understanding of the substituent effects (i.e., steric or electronic) on the chromophore light-induced dynamics. In the present letter we compare the results of quantum mechanics/molecular mechanics excited-state trajectories of native and analogue-hosting microbial rhodopsins from the eubacterium *Anabaena*. The results uncover a relationship between the nature of the substituent on the analogue (i.e., electron-donating (a Me group) or electron-withdrawing (a CF_3 group)) and rhodopsin excited-state lifetime. Most importantly, we show that electron-donating or -withdrawing substituents cause a decrease or an increase in the electronic mixing of the first two excited states which, in turn, controls the photoisomerization speed.

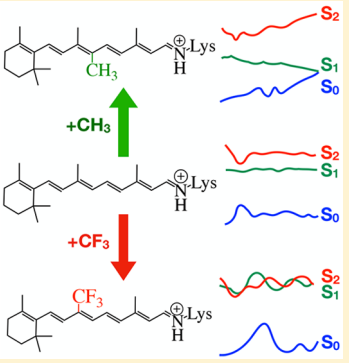

The use of retinal proteins (simply, rhodopsins) hosting synthetic retinal protonated Schiff base (rPSB) analogues in optogenetics and fluorescence microscopy is receiving increasing attention.[1,2] Such analogues not only allow achieving long wavelength sensitivity, which is essential for the biological applications,[3] but also provide a way of engineering fast or slow photoreactivity into the protein. In principle, the latter is highly important, especially in designing rhodopsin-based fluorescent probes where one should hinder the isomerization of rPSB in order to achieve a higher excited-state lifetime and therefore a higher fluorescence.[4,5] Thus, understanding the impact of different rPSB substituents on absorption wavelength and photoisomerization time scale is of great importance. While the wavelength tuning is often achieved by increasing the π-system of the rPSB or introducing electron-donating or -withdrawing substituents, controlling the photoreactivity using such strategies requires a better understanding of their effects on the rPSB photodynamics. More specifically, one must understand which effects of the substitution (i.e., electronic, steric, etc.) cause a change in the photodynamics. Among the recent studies aiming to achieve such knowledge, the works by Kukura et al. and Garavelli et al. are significant.[6−8] Kukura et al. investigated the photoisomerization of several artificial rPSB pigments in methanol solution using time-resolved spectroscopy.[6,7] An interesting result from their experiments is that the introduction of a Me group at the C10 position (10Me-rPSB) of the native rPSB backbone (see Scheme 1A) red-shifted the absorption wavelength by only a few nanometers but decreased the original excited-state lifetime from 4 to 0.7 ps. Later, Garavelli et al. reported a computational study indicating that the fast decay of 10Me-rPSB in solution is the result of an electron-releasing effect of the Me substituent that increases the energy gap between the first (S_1) and second (S_2) electronic singlet excited states.[8] While the above investigations have provided basic information on rPSB photoreactivity tuning in solution, no information is presently available on the chromophore analogue control of the photoisomerization inside the protein environment (termed opsin cavity in the following). In the past, bacteriorhodopsin (bR) hosting different artificial rPSB pigments has been employed in various experimental studies.[9−13] One such study provided evidence that electron-withdrawing groups such as CF_3 inhibit the photoisomerization.[10] However, a computational/mechanistic study looking at which specific effects (i.e., steric or electronic) speed up or slow down the rPSB photoisomerization in the opsin cavity remains unreported.

We demonstrate how electronic effects introduced by Me or CF_3 in specific positions of the all-*trans* rPSB chromophore backbone control the photoreactivity of rPSB inside the opsin cavity. To do so, we construct hybrid quantum mechanics/molecular mechanics (QM/MM) models of a selected

Received: August 18, 2018
Accepted: October 18, 2018
Published: October 18, 2018

DOI: 10.1021/acs.jpclett.8b02550
J. Phys. Chem. Lett. 2018, 9, 6350−6355

Scheme 1. PESs and the Associated Electronic Characters of ASR_{AT} Models at the FC Point[a]

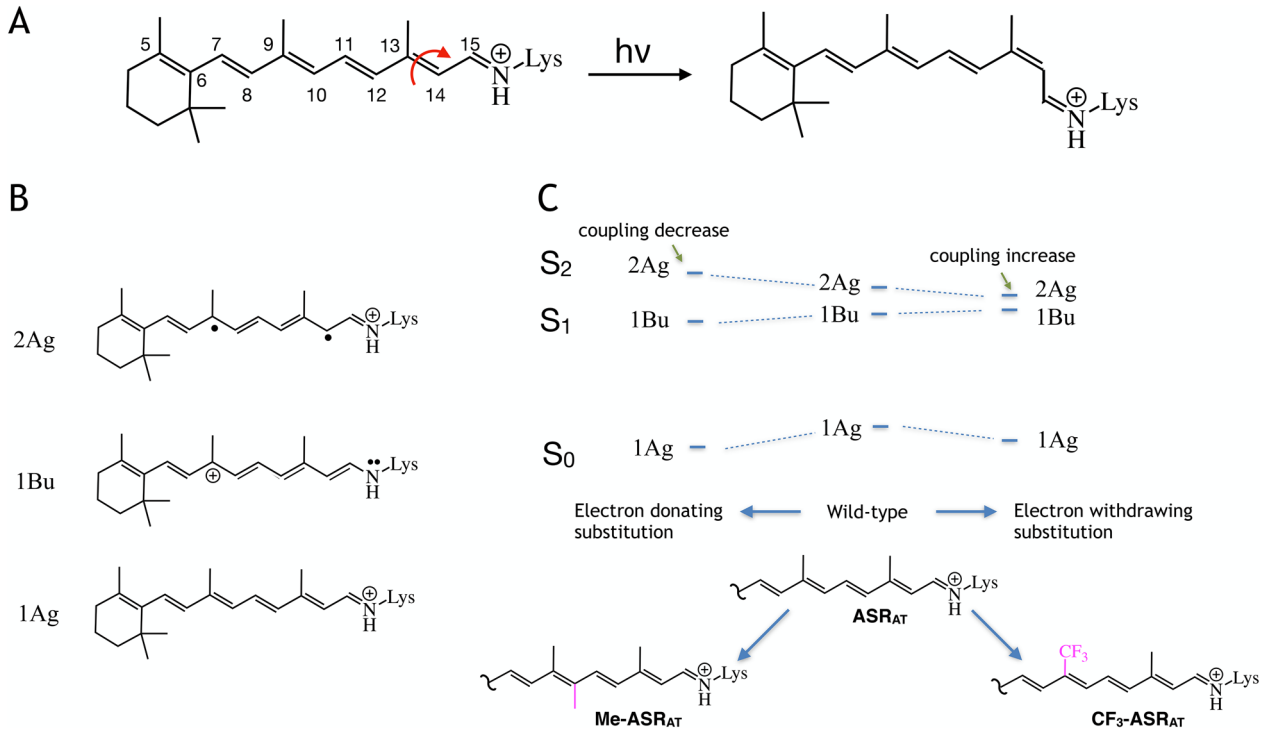

[a](A) Structure of the native all-*trans* rPSB chromophore and representation of its photoisomerization reaction to the 13-*cis* rPSB chromophore. (B) Resonance structures showing the electronic characters dominating the S_0 (bottom), S_1 (middle), and S_2 (top) states of ASR_{AT} in its vertical excitation region (also called FC region). (C) Schematic representation of the effect of electron-releasing (10-methyl, Me-ASR_{AT}) or -withdrawing (9-trifluoromethyl, CF3-ASR_{AT}) substituents on the relationship between the PESs of ASR_{AT} at the FC region.

microbial opsin with native and artificial rPSBs featuring electron-releasing or -withdrawing substituents. The selected rhodopsin, *Anabaena* sensory rhodopsin (ASR), is found in the fresh water cyanobacterium *Anabaena* (Nostoc) PCC7120 and is known to naturally host both all-*trans* and 13-*cis* rPSBs (hereafter ASR_{AT} and ASR_{13C}).[14,15] As convenient rPSB analogues, we have chosen 10-methylated and 9-trifluoromethylated all-*trans* and 13-*cis* rPSBs. Hereafter, ASR hosting these rPSB analogues will be termed Me-ASR_X and CF3-ASR_X, respectively, where X stands for AT or 13C. The corresponding QM/MM models are then used to compute the wavelength of the absorption maximum (λ_{max}) of each rhodopsin. More explicitly, we compute the corresponding vertical excitation energies at the Franck−Condon (FC) points. The same models are then used to investigate their photoisomerization dynamics. More specifically, QM/MM models are used to simulate the photodynamics of rPSB along short (<150 fs long) trajectories initiated on S_1 or S_2 potential energy surface (PES) with zero kinetic energies (FC trajectories, see the Supporting Information for details). We assume that in a subpicosecond time scale, FC trajectories represent the center of a vibrational wave packet and thus provide information on the population dynamics. This assumption is supported by our previous photodynamics studies.[16,17]

In our QM/MM photodynamics simulations, geometrical progression is computed using 3-root-state-averaged CASSCF/AMBER gradients.[18] The effect of dynamic electron correlation is then introduced by recomputing the S_0, S_1, and S_2 energy profiles at the CASPT2[19] level of theory.

Substituent Effects on λ_{max} Originate from Competing Steric and Electronic Effects. We employ the ASR_{AT}, Me-ASR_{AT}, and CF3-ASR_{AT} models to look at the absorption spectroscopy of the corresponding rhodopsins. However, before discussing the computational results, it is necessary to revise our general understanding on the excited states of the rPSB chromophore. As depicted in Scheme 1B, the electronic structures (termed "characters") contributing to the 3-root-state-average wave functions (S_0, S_1, and S_2) of each model are termed 1Ag (covalent), 1Bu (charge transfer), and 2Ag (diradical), respectively.[16,17,20] In ASR_{AT}, the S_0 PES at the FC point displays dominating 1Ag character where the positive charge of the chromophore is mostly distributed in the Schiff base (−CH=NH−) region. At the same location, the S_1 and S_2 PESs display dominating 1Bu and 2Ag characters, respectively. Therefore, S_1 is characterized by the majority of the positive charge located in the β-ionone side of the rPSB, and it is reactive as the S_0 double bonds have become, effectively, single bonds. On the other hand, S_2 displays a charge distribution similar to that of the covalent S_0 state with the charge mainly residing on the Schiff base moiety, and it is not reactive as the double bonds still have bonding character.

As illustrated in Scheme 1C (see the computed vertical excitation energies in Table S1 for the numerical values), the introduction of electron-releasing or -withdrawing substituents leads to a relative stabilization or destabilization of the three different PESs. In fact, 9-trifluoromethylation destabilizes the S_1 PES with respect to the S_0 PES because of its 1Bu character and, for the same reason, decreases the S_2-S_1 gap. Consistently, the introduction of an electron-donating substituent (Me-ASR_{AT}) results in an increased S_1-S_2 energy

DOI: 10.1021/acs.jpclett.8b02550
J. Phys. Chem. Lett. 2018, 9, 6350−6355

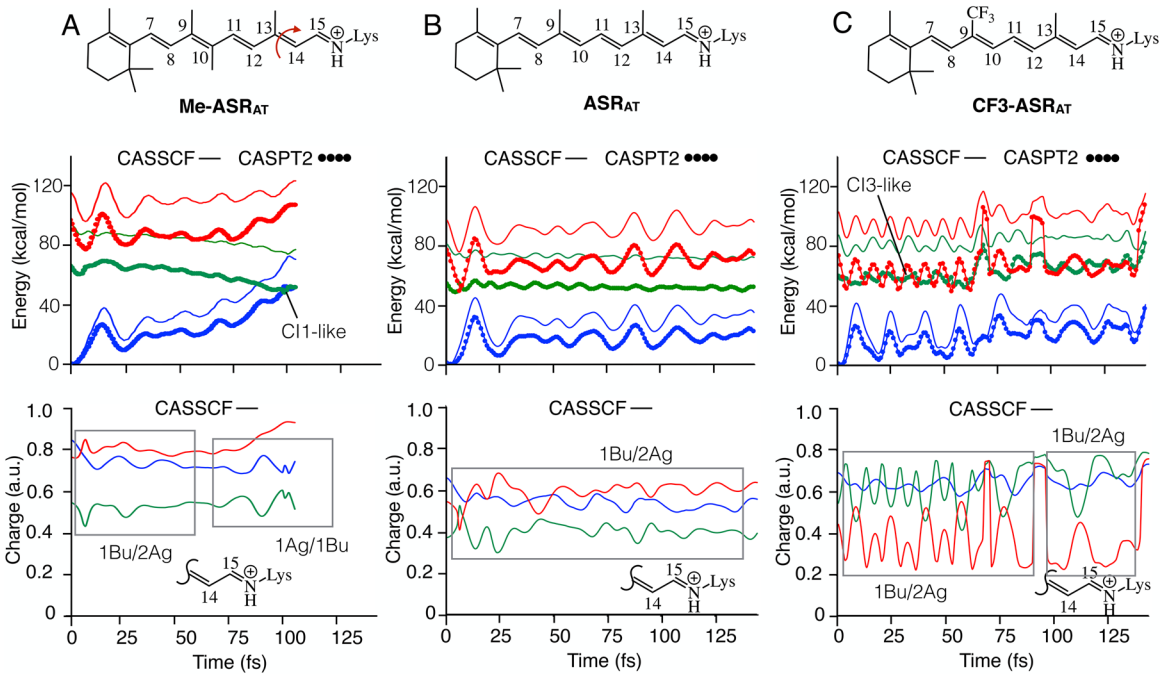

Figure 1. Substituent effect on the relaxation of ASR$_{AT}$. (A) CASSCF and CASPT2 energy profiles (top panel) and evolution of CASSCF charge on the Schiff base side (bottom panel) of the Me-ASR$_{AT}$. (B) Same data for ASR$_{AT}$. (C) Same data for CF3-ASR$_{AT}$. S_0, S_1, and S_2 PESs are shown in blue, green, and red, respectively. The profiles shown in the bottom panels report the value of the positive charge on the displayed molecular fragment.

gap. However, contrary to what is expected on the basis of electronic effects, we observe an increase in the S_0-S_1 excitation energy with respect to the rhodopsin with the native chromophore. This is due to steric effects. In fact, we find that the 10-methyl substituted rPSB becomes highly distorted around C6−C7 and C8−C9 single bonds (see Figure S2A), leading to partial deconjugation and, therefore, a λ_{max} blue-shift.

As we have discussed so far, addition of electron-donating or -withdrawing groups change the S_1-S_2 energy gap of PESs in the FC region. Below we show that such substitutions also lead to character variation along the S_1 trajectory driving the photoisomerization of ASR$_{AT}$ to ASR$_{13C}$ (see Figure 1) by decreasing or increasing the reactive 1Bu or unreactive 2Ag character. At this stage, it is essential to note three important pieces of information that we fully detailed in ref 17: (1) The shape of the rPSB CASPT2 and CASSCF energy profiles are similar. (2) During the rPSB S_1 relaxation starting at the FC point, the system may reach two conical intersections, namely CI1 and CI3, where the first is a crossing between the S_1 and S_0 PESs associated with the 1Bu and 1Ag characters, while the second is a crossing between the S_2 and S_1 PESs associated with the 2Ag and 1Bu characters (a third conical intersection, CI2, between PESs dominated by 1Ag and 2Ag is higher in energy and it is not involved in rPSB photodynamics). (3) The change in the total charge of a suitable rPSB moiety can be used to learn about the magnitude of the coupling between different PESs.

In Figure 1, we present the results of our FC trajectory computations for ASR$_{AT}$ with and without retinal analogues. These include the evolution of the CASSCF and CASPT2 energies and of the total CASSCF Mulliken charges on a selected moiety of the chromophore (the Schiff base moiety −C14H−C15H=NH−). Note that such charges were computed at the CASSCF level to be consistent with geometrical progression.

Electron-Releasing Substitution Reduces the 1Bu/2Ag Mixing and Leads to a Faster Rhodopsin Photoisomerization. The results presented in Figure 1 are interpreted using the information given in points 1−3 above. Upon inspection of the energy profiles one notes that in the case of ASR$_{AT}$ (Figure 1B, central panel) the molecule remains on S_1 for the whole simulation time. This observation is consistent with the fact that ASR$_{AT}$ decay takes more than 700 fs experimentally, as reported by previous investigations.[21,22] The charge variation displayed in Figure 1B (bottom panel) shows that the Schiff base moiety of the rPSB carries an oscillating positive charge centered around ∼0.6 on both S_2 and S_0 states and ∼0.4 charge on the S_1 state. Recall that a large positive charge on the Schiff base moiety indicates a 1Ag or 2Ag character and that a small charge indicates 1Bu character. Thus, in conclusion, the S_1 PES displays an oscillating 1Bu character. These oscillations exhibit an out-of-phase relationship with oscillations of S_2 PES that is associated with the 2Ag character (see the framed region in Figure 1B bottom panel). Such a relationship indicates that S_1 and S_2 PESs are interacting with each other (i.e., the two states feature mixed 2Ag and 1Bu characters) and the S_1 PES is only "partially" reactive.

As apparent from Figure 1A, the above situation changes upon addition of a 10-methyl group in Me-ASR$_{AT}$. The oscillatory relationship between S_1 and S_2 characters lasts only for about 60 fs, and thereafter, S_1 displays an out-of-phase oscillation relationship with the S_0 PES. This means that, after 60 fs relaxation, the S_1 PES is interacting with S_0 mixing 1Bu and 1Ag characters and continues until the molecule reaches CI1 and decays to S_0 at 110 fs, eventually producing the 13-*cis* isomer. The slow decay of ASR$_{AT}$ and the fast decay of Me-ASR$_{AT}$ are consistent with the changes documented between

DOI: 10.1021/acs.jpclett.8b02550
J. Phys. Chem. Lett. 2018, 9, 6350−6355

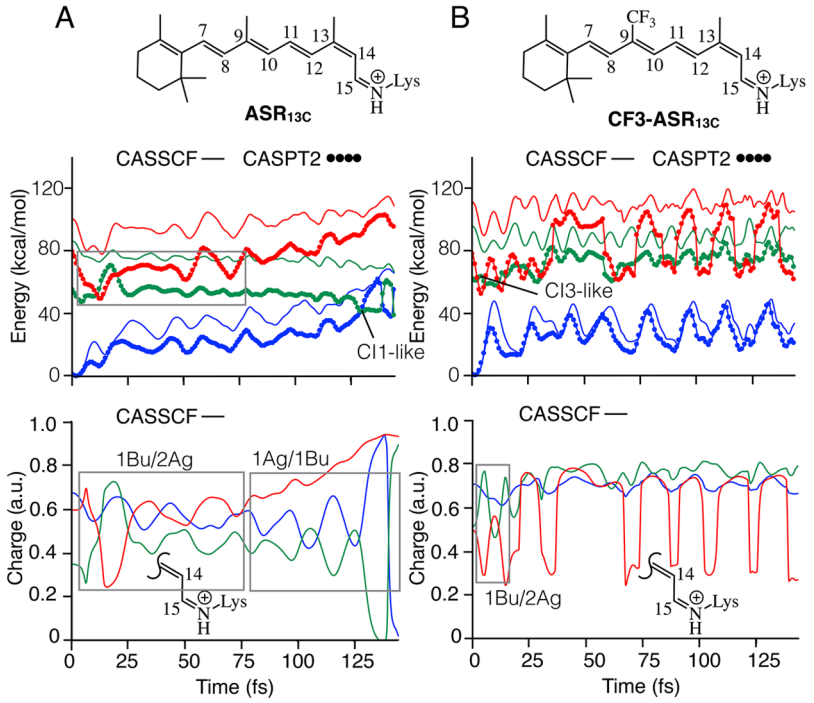

Figure 2. Effect of CF3 substitution on the relaxation of ASR_{13C}. (A) CASSCF and CASPT2 energy profiles (top panel) and evolution of the charge on the Schiff base side (bottom panel) of ASR_{13C}. (B) Same data for CF3-ASR_{13C}. S_0, S_1, and S_2 PESs are shown in blue, green, and red, respectively. The profiles shown in the bottom panels report the value of the positive charge on the displayed molecular fragment.

all-*trans*-rPSB and 10Me-rPSB in methanol solution.[6,8] In conclusion, in the protein cavity, the 10-Me substituent induces the same effect seen in solution.

Electron-Withdrawing Substituents Increase 1Bu/2Ag Mixing, Which May Lead to a Slower (or Blocked) Photoisomerization. Comparison of panels B and C of Figure 1 shows that replacing the methyl group at C9 position with a CF3 leads to strong S_2/S_1 state mixing. At the FC point of CF3-ASR_{AT}, the optically allowed 1Bu-like state is slightly higher in energy than the 2Ag-like state (i.e. the spectroscopic state corresponds to S_2 rather than S_1). This is observed in both CASSCF and CASPT2 energy profiles. The CF3-ASR_{AT} relaxation along the S_1 PES leads, within 62 fs, to a CI3-like structure with mixed 1Bu/2Ag character which may hop to the S_2 PES. From S_2, the system may then return to S_1 through another CI3-like conical intersection leading to an oscillatory 1Bu/2Ag character. Another interpretation would be that the system remains on the S_1 PES but features a bumpy motion with frequent changes between reactive (1Bu) and unreactive (2Ag) electronic character, thus slowing down the isomerization motion. More specifically, the strong state mixing results in an adiabatic S_1 potential energy surface featuring an avoided crossing between diabatic states with covalent (2Ag) and charge transfer (1Bu) characters. Thus, the observed molecular motion on the S_1 PES would correspond to attempts to overcome a barrier (generated by the avoided crossing between S_2 and S_1) resulting in a slower photoreactivity (see Figure S3). It is important to note that S_1 and S_2 CASPT2 energy profiles show a similar shape to CASSCF until the S_1 to S_2 hop point but exhibit different shapes thereafter. Further inspection of the CASPT2 energy profiles show sudden increases in energy around 65 and 85 fs of the trajectory. This indicates that the S_1 PES interacts with a higher excited-state PES as supported by the inspection of the charge profiles. In fact, during the first ∼90 fs of the CF3-ASR_{AT} relaxation, we observe a dominating out-of-phase relationship between S_1 and S_2 charge profiles (1Bu/2Ag state mixing) similar to ASR_{AT}. However, such relationship occasionally disappears, and this is attributed to a coupling with another higher state. In order to track the interacting higher state, we recomputed energy and charge profiles at the 4-root-state-average level along the same geometries. The results indicate that the S_3 PES is interacting with S_1 (see Figure S4). On the basis of the above results, we predict that the electron-withdrawing group that we have introduced has increased state mixing of rPSB, resulting in a longer decay time with respect to ASR_{AT}. In order to better demonstrate the increase in decay time, we propagated a ASR_{13C} trajectory. In fact, ASR_{13C} that incorporates a native 13-*cis* chromophore has an observed excited-state lifetime of ca. 150 fs.[21] As apparent from inspection of Figure 2A, our ASR_{13C} model decays to the ground state within 150 fs, consistently with previous theoretical and experimental studies.[16,21] Inspection of charge profiles suggests that 1Bu/2Ag mixing persists until about 75 fs, and then 1Bu/1Ag mixing takes over until the hop point (see framed regions in the bottom panel). Such a situation is completely different from that found after introduction of CF3. In fact, the FC region of CF3-ASR_{13C} displays similar features to the CF3-ASR_{AT}, and the relaxation initiates from a S_2 PES, which is dominated by the 1Bu character. The first ∼15 fs of relaxation are dominated by 1Bu/2Ag mixing, but the molecule reaches a CI3-like point and hops to the S_1 PES which is associated with unreactive 2Ag character. During this time, the S_1 PES appears to interact with another state. This is evident from the absence of a 1Bu-like state that displays an out-of-phase relationship with the 2Ag-like state (see Figure 2B, bottom panel). Recomputing the energies at 4-root-state-average level suggests that the interacting PES is S_3 (see Figure S4). The unreactive 2Ag character associated with S_1 PES explains why CF3-ASR_{13C} does not undergo isomerization similar to ASR_{13C}.

DOI: 10.1021/acs.jpclett.8b02550
J. Phys. Chem. Lett. 2018, 9, 6350−6355

More specifically, 9-trifluoromethylation has contributed to an increase in the electronic state mixing of ASR_{13C}.

In the past, the effect of 9-trifluoromethylation on bR (CF3-bR) photoisomerization has been experimentally documented by Ottolenghi, Sheves and co-workers.[10] In such work, the authors carried out steady-state absorption experiments and second harmonic generation experiments of CF3-bR and native bR. The formation of photoproduct intermediates was also studied. The results showed that the CF3-bR absorption maximum is blue-shifted by 48 nm with respect to bR. Furthermore, the second harmonic generation signal of the former (0.375) was significantly low with respect to the latter (1.0). However, the authors observed photoproduct intermediates in both cases. The fact that the calculated absorption maxima of CF3-ASR_{AT} and CF3-ASR_{13C} above are blue-shifted with respect to their native counterparts is consistent with the results of bR absorption experiments. We also constructed QM/MM models for CF3-bR and bR and studied the absorption spectroscopic properties. Consistently with the experiments, the computed maximum absorption wavelength of the former is blue-shifted by 66 nm in comparison to the latter (see Table S1). At the FC region, the S_1-S_2 energy gaps of both models remain close to each other; however, the increased S_1/S_2 mixing of CF3-bR is clearly evident as the molecule is allowed to relax on S_1 PES (see Figure S5).

Considerations for Designing Artificial rPSB Analogues Useful in High-Resolution Imaging. Above, we provided computational evidence for a correlation between the type of rPSB substitutions (i.e., electron-withdrawing or -donating) and electronic state mixing. More specifically, a microbial rhodopsin hosting an electron-releasing, native, and electron-withdrawing rPSBs display low, moderate, and high amounts of state mixing, respectively. The corresponding decay times increase as we go from electron-rich rPSB to electron-poor rPSB. The relationship that we have reported here may be used as a design principle to develop rPSB chromophore analogues that, after insertion into a suitable opsin, would provide fluorescent probes useful in high-resolution imaging. In fact, as reported in the literature, creating an excited-state barrier and preventing the photoisomerization of rPSB is a way of engineering fluorescence into a rhodopsin.[4] Because increasing electronic state mixing appears to hinder the photoisomerization, we propose searching for other electron-withdrawing substituents and suitable substitution positions on the chromophore chain to increase the electronic state mixing of rPSB as another way of engineering fluorescence. According to the results presented above, ASR_{AT} is a potential candidate for such reengineering resulting in novel fluorescent probes.

■ ASSOCIATED CONTENT

Supporting Information

The Supporting Information is available free of charge on the ACS Publications website at DOI: 10.1021/acs.jpclett.8b02550.

> Methodology, absorption energies and oscillator strengths, comparison of rPSB geometries and cavity residues of ASR_{AT} models, evolution of a molecule through a bumpy PES formed by avoided crossings, energy profiles computed at 4-root-state-average level, and energy and charge profiles of bR models (PDF)

■ AUTHOR INFORMATION

Corresponding Author

*E-mail: molivuc@bgsu.edu.

ORCID

Madushanka Manathunga: 0000-0002-3594-8112

Massimo Olivucci: 0000-0002-8247-209X

Notes

The authors declare no competing financial interest.

■ ACKNOWLEDGMENTS

This work was supported in part by the Italian MIUR for funding (PRIN 2015) and, in part, by the National Science Foundation under Grant No. CHE-1710191 and National Institute of Health under Grant No. R15GM126627. M.O. is grateful to USIAS (University of Strasbourg) for a 2015 fellowship and to the Ohio Supercomputer Center for granting computer time. We are also grateful to Dr. Alessio Valentini for useful discussions.

■ REFERENCES

(1) AzimiHashemi, N.; Erbguth, K.; Vogt, A.; Riemensperger, T.; Rauch, E.; Woodmansee, D.; Nagpal, J.; Brauner, M.; Sheves, M.; Fiala, A.; et al. Synthetic Retinal Analogues Modify the Spectral and Kinetic Characteristics of Microbial Rhodopsin Optogenetic Tools. *Nat. Commun.* **2014**, *5*, 5810.

(2) Herwig, L.; Rice, A. J.; Bedbrook, C. N.; Zhang, R. K.; Lignell, A.; Cahn, J. K. B.; Renata, H.; Dodani, S. C.; Cho, I.; Cai, L.; et al. Directed Evolution of a Bright Near-Infrared Fluorescent Rhodopsin Using a Synthetic Chromophore. *Cell Chem. Biol.* **2017**, *24*, 415−425.

(3) Sineshchekov, O. A.; Govorunova, E. G.; Wang, J.; Spudich, J. L. Enhancement of the Long-Wavelength Sensitivity of Optogenetic Microbial Rhodopsins by 3,4-Dehydroretinal. *Biochemistry* **2012**, *51*, 4499−4506.

(4) Laricheva, E. N.; Gozem, S.; Rinaldi, S.; Melaccio, F.; Valentini, A.; Olivucci, M. Origin of Fluorescence in 11-Cis Locked Bovine Rhodopsin. *J. Chem. Theory Comput.* **2012**, *8*, 2559−2563.

(5) Kandori, H.; Katsuta, Y.; Ito, M.; Sasabe, H. Femtosecond Fluorescence Study of the Rhodopsin Chromophore in Solution. *J. Am. Chem. Soc.* **1995**, *117*, 2669−2670.

(6) Sovdat, T.; Bassolino, G.; Liebel, M.; Schnedermann, C.; Fletcher, S. P.; Kukura, P. Backbone Modification of Retinal Induces Protein-like Excited State Dynamics in Solution. *J. Am. Chem. Soc.* **2012**, *134*, 8318−8320.

(7) Bassolino, G.; Sovdat, T.; Liebel, M.; Schnedermann, C.; Odell, B.; Claridge, T. D. W.; Kukura, P.; Fletcher, S. P. Synthetic Control of Retinal Photochemistry and Photophysics in Solution. *J. Am. Chem. Soc.* **2014**, *136*, 2650−2658.

(8) Demoulin, B.; Altavilla, S. F.; Rivalta, I.; Garavelli, M. Fine Tuning of Retinal Photoinduced Decay in Solution. *J. Phys. Chem. Lett.* **2017**, *8*, 4407−4412.

(9) Bayley, H.; Radhakrishnan, R.; Huang, K. S.; Khorana, H. G. Light-Driven Proton Translocation by Bacteriorhodopsin Reconstituted with the Phenyl Analog of Retinal. *J. Biol. Chem.* **1981**, *256*, 3797−3801.

(10) Zadok, U.; Khatchatouriants, A.; Lewis, A.; Ottolenghi, M.; Sheves, M. Light-Induced Charge Redistribution in the Retinal Chromophore Is Required for Initiating the Bacteriorhodopsin Photocycle. *J. Am. Chem. Soc.* **2002**, *124*, 11844−11845.

(11) Ottolenghi, M.; Sheves, M. Synthetic Retinals as Probes for the Binding Site and Photoreactions in Rhodopsins. *J. Membr. Biol.* **1989**, *112*, 193−212.

(12) Sheves, M.; Albeck, A.; Friedman, N.; Ottolenghi, M. Controlling the PKa of the Bacteriorhodopsin Schiff Base by Use of Artificial Retinal Analogues. *Proc. Natl. Acad. Sci. U. S. A.* **1986**, *83*, 3262−3266.

DOI: 10.1021/acs.jpclett.8b02550
J. Phys. Chem. Lett. 2018, 9, 6350−6355

(13) Albeck, A.; Friedman, N.; Sheves, M.; Ottolenghi, M. Factors Affecting the Absorption Maxima of Acidic Forms of Bacteriorhodopsin. A Study with Artificial Pigments. *Biophys. J.* **1989**, *56*, 1259−1265.
(14) Jung, K.-H.; Trivedi, V. D.; Spudich, J. L. Demonstration of a Sensory Rhodopsin in Eubacteria. *Mol. Microbiol.* **2003**, *47*, 1513−1522.
(15) Schapiro, I.; Ruhman, S. Ultrafast Photochemistry of Anabaena Sensory Rhodopsin: Experiment and Theory. *Biochim. Biophys. Acta, Bioenerg.* **2014**, *1837*, 589−597.
(16) Luk, H. L.; Melaccio, F.; Rinaldi, S.; Gozem, S.; Olivucci, M. Molecular Bases for the Selection of the Chromophore of Animal Rhodopsins. *Proc. Natl. Acad. Sci. U. S. A.* **2015**, *112*, 15297−15302.
(17) Manathunga, M.; Yang, X.; Orozco-Gonzalez, Y.; Olivucci, M. Impact of Electronic State Mixing on the Photoisomerization Timescale of the Retinal Chromophore. *J. Phys. Chem. Lett.* **2017**, *8*, 5222−5227.
(18) Frutos, L. M.; Andruniów, T.; Santoro, F.; Ferré, N.; Olivucci, M. Tracking the Excited-State Time Evolution of the Visual Pigment with Multiconfigurational Quantum Chemistry. *Proc. Natl. Acad. Sci. U. S. A.* **2007**, *104*, 7764−7769.
(19) Andersson, K.; Malmqvist, P.-Å.; Roos, B. O. Second-Order Perturbation Theory with a Complete Active Space Self-Consistent Field Reference Function. *J. Chem. Phys.* **1992**, *96*, 1218−1226.
(20) Gozem, S.; Luk, H. L.; Schapiro, I.; Olivucci, M. Theory and Simulation of the Ultrafast Double-Bond Isomerization of Biological Chromophores. *Chem. Rev.* **2017**, *117*, 13502−13565.
(21) Cheminal, A.; Leonard, J.; Kim, S.-Y.; Jung, K.-H.; Kandori, H.; Haacke, S. 100 fs Photo-Isomerization with Vibrational Coherences but Low Quantum Yield in Anabaena Sensory Rhodopsin. *Phys. Chem. Chem. Phys.* **2015**, *17*, 25429−25439.
(22) Wand, A.; Rozin, R.; Eliash, T.; Jung, K.-H. H.; Sheves, M.; Ruhman, S. Asymmetric Toggling of a Natural Photoswitch: Ultrafast Spectroscopy of Anabaena Sensory Rhodopsin. *J. Am. Chem. Soc.* **2011**, *133*, 20922−20932.

DOI: 10.1021/acs.jpclett.8b02550
J. Phys. Chem. Lett. 2018, 9, 6350−6355